

Quantifying Heat Transfer in DMD-based Optoelectronic Tweezers with Infrared Thermography

Peter J. Pauzauskie*^a, Hsan-Yin Hsu^b, Arash Jamshidi^b, Justin K. Valley^b,
Shao Ning Pei^b, Ming C. Wu^b

^aChemical Sciences Division, Lawrence Livermore National Laboratory, Livermore, CA 94551;

^bDepartment of Electrical Engineering, University of California, Berkeley, Berkeley, CA, 94720

ABSTRACT

Optoelectronic tweezers (OET) have emerged in recent years as a powerful form of optically-induced dielectrophoresis for addressing single cells and trapping individual nanostructures with DMD-based virtual-electrodes. In this technique an alternating electric field is used to induce a dipole within structures of interest while very low-intensity optical images are used to produce local electric field gradients that create dynamic trapping potentials. Addressing living cells, particularly for heat-sensitive cell lines, with OET's optical virtual-electrodes requires an in-depth understanding of heating profiles within OET devices. In this work we present quantitative measurements of the thermal characteristics of single-crystalline-silicon phototransistor based optoelectronic tweezers (PhOET). Midwave infrared (3 – 5 micron) thermographic imaging is used to determine relative heating in PhOET devices both with and without DMD-based optical actuation. Temperature increases of approximately 2°C from electrolyte Joule-heating are observable in the absence of DMD-illumination when glass is used as a support for PhOET devices. An additional temperature increase of no more than 0.2°C is observed when DMD-illumination is used. Furthermore, significantly reduced heating can be achieved when devices are fabricated in direct contact with a metallic heat-sink.

Keywords: optoelectronic tweezers, dielectrophoresis, optical manipulation, thermography, heat transfer

1. INTRODUCTION

The first demonstration of single-beam laser tweezers in the 1970's sparked a flood of interest in non-contact, optical manipulation of micron-scale particles^{1,2}. In this technique a highly-focused beam (commonly in the near-infrared) is used to create three-dimensional trapping potentials that have led to a revolution in the optical manipulation of matter³. A broad range of structures have been trapped including individual cells⁴, micron-scale dielectric particles^{5,6}, as well as sub-micron particles including inorganic nanowires^{7,8} and carbon nanotubes⁹⁻¹¹. Additionally, stable trapping has been demonstrated for a range of sub-micron biological structures including viruses¹² and individual organelles¹³. Tethering biological macromolecules to dielectric spheres has evolved into a highly sensitive probe of the forces encountered by motor proteins including viral DNA packaging structures¹⁴ as well as the torsional properties of the kinesin transport system¹⁵.

In order to achieve stable trapping with laser tweezers the laser's intensity must be high enough for the coherent laser light to polarize the dielectric particle of interest. Forces result when the particle's induced dipole interacts with the local inhomogeneous electric field that is created when the laser is focused to a diffraction-limited spot. The intensities used commonly range from 0.1 to 1MW/cm² which is high enough for non-linear effects such as frequency doubling of the trapping laser¹⁶⁻¹⁸. One consequence of these high optical intensities is that even small absorption coefficients can result in a significant amount of photodamage¹⁹. For metallic structures, the damage is largely thermal from free-carrier absorption²⁰, while in biological systems the photo-damage has been correlated with the local generation of highly-reactive singlet oxygen²¹ as well as heating²². Furthermore, the large optical intensities and high numerical-aperture objectives required for creating optical traps also restrict the active working area of a given instrument to be on the order of 100 μm.

*pauzauskie1@llnl.gov; phone 1 925 422-7319

Emerging Digital Micromirror Device Based Systems and Applications II, edited by Michael R. Douglass, Larry J. Hornbeck,
Proc. of SPIE Vol. 7596, 759609 · © 2010 SPIE · CCC code: 0277-786X/10/\$18 · doi: 10.1117/12.846247

Proc. of SPIE Vol. 7596 759609-1

Dielectrophoresis²³ (DEP) is another form of non-contact nanomanipulation in which lithographically patterned metallic electrodes are used to create dipoles within particles as well as inhomogeneous electric fields resulting in forces on the particles. This technique has been used to great effect to trap living cells and submicron structures for a variety of different applications in particle sorting, assembly, and characterization²⁴⁻²⁶. However, metallic microelectrodes cannot create arbitrary trapping potentials in real time given that the position of the electrodes cannot be modified after microfabrication. CMOS based DEP chips have been used to improve spatial resolution for DEP-based manipulation of individual cells²⁷ although the ultimate spatial resolution is limited by lithography to the micron scale.

Optoelectronic tweezers have been developed in recent years as a platform that combines the massive parallelism of DEP with the optical flexibility of laser tweezers²⁸⁻³⁰. Particles of interest are sandwiched between parallel-plate electrodes with the top electrode normally consisting of a transparent conducting indium-tin-oxide (ITO) thin film deposited on a glass coverslip. The bottom electrode consists of either a hydrogenated amorphous silicon (a-Si:H) thin film photoconductor deposited on another ITO-glass coverslip or an array of bipolar junction phototransistors in single crystalline silicon (Figure 1). An AC electric field is applied across the parallel plate capacitor that induces dipole moments within the particles sandwiched between the electrodes (Figure 1). Large photoconductive gain in the silicon enables incoherent light to change the silicon's impedance by several orders of magnitude. In this way, low-intensity optical images from DLP® projectors can be used to illuminate the photoconductor over large areas, leading to significant electric field gradients that are spatially controlled by the optical image. The approach can be thought of as a form of light-induced DEP where the AC electric fields across the parallel plate electrodes control dipole formation while optical illumination of the photoconductor dictates when and where electric field gradients are established.

To date the approach has been used for several processes involving live cells including dynamic manipulation²⁹⁻³³, discrimination and sorting^{34, 35}, as well as selective electroporation³⁶. OET has also been used to address submicron structures such as inorganic nanowires³⁷⁻⁴⁰, DNA tethered to dielectric beads⁴¹, gold nanocrystals³⁵, and multiwalled carbon nanotubes⁴². For many biological applications the temperature of the liquid electrolyte medium is an important parameter that must be controlled to ensure cellular viability⁴³. In this paper we use infrared thermography in tandem with finite element simulations to characterize the thermal performance of DLP®-based OET devices with the goal of ensuring optimal thermal management for a range of cellular trapping, sorting, and culturing experiments.

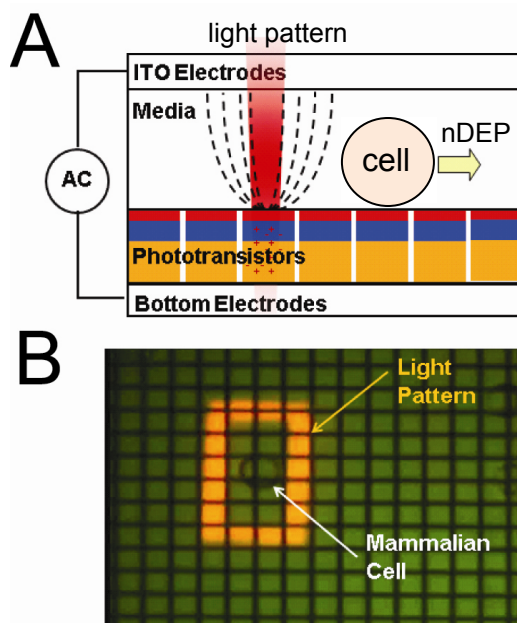


Figure 1. (A) Schematic of PhOET chamber configuration. Low intensity optical images are used to create electric field gradients which produce forces on polarized micron-scale structures such as living cells. Repulsive negative dielectrophoresis (nDEP) is usually observed for cells with PhOET. The bottom electrodes are either in direct contact with a thermoelectric cooling stage or insulated by a 1 mm thick glass coverslip. (B) 20X visible light microscope image of a mammalian cell (HeLa) confined in a square trapping region produced from an optical projector.

2. EXPERIMENTAL CONFIGURATION

The PhOET device (Figure 1) is designed to operate using physiologically relevant electrolyte conductivities, typically between 0.5 and 1.5 S/m while the OET device is designed to work at lower electrolyte conductivities commonly encountered in cell electroporation. A function generator (Agilent) and amplifier (TEGAM #2348) are used to apply voltages ranging from 1 to 40 Vpp, at frequencies ranging between 100kHz to 1 MHz. Normally ~10 μ L of 1M phosphate buffered saline (PBS, $\sigma=1.4$ S/m) electrolyte solution is loaded into the PhOET device. Adhesive spacers are used to set the liquid layer thickness at approximately 100 μ m. The chamber is then placed on the temperature stage for calibration with the thermographic camera.

The experimental thermography apparatus (Figure 2) consists of a DMD-based OET system with the active photoconductor being either bipolar junction phototransistors in single crystalline silicon (PhOET)⁴⁴ or hydrogenated amorphous silicon deposited through plasma-enhanced chemical vapor deposition (OET)³⁰. A DLP® projector is used to produce optical images that are focused through a 20x visible objective lens (Mitutoyo). Device temperatures are monitored by a mid-wave infrared thermography camera. The camera (FLIR, HS4000) consists of a 320 x 256 pixel InSb focal plane array (30 μ m pixel pitch) sensitive to infrared photons within the 3 – 5 μ m spectral band. The camera's field of view is ~3 cm with a spatial resolution of ~100 μ m. The camera integration time is kept constant at 9 μ s throughout all measurements. The stage temperature is regulated by a thermoelectric PID controller with a range between 20 and 50°C.

The PhOET chamber's top surface is a 1mm thick layer of silica glass that has an approximately Lambertian thermal infrared emission profile for viewing angles below 50°. Care was taken in all measurements to ensure the viewing angle θ was below 50°. The stage temperature is set to a specific value and allowed to come into thermal equilibrium with the PhOET device. The thermographic camera is used to record sequential images to determine when the stage and device reach a series of steady state temperatures ranging from 20°C to 50°C.

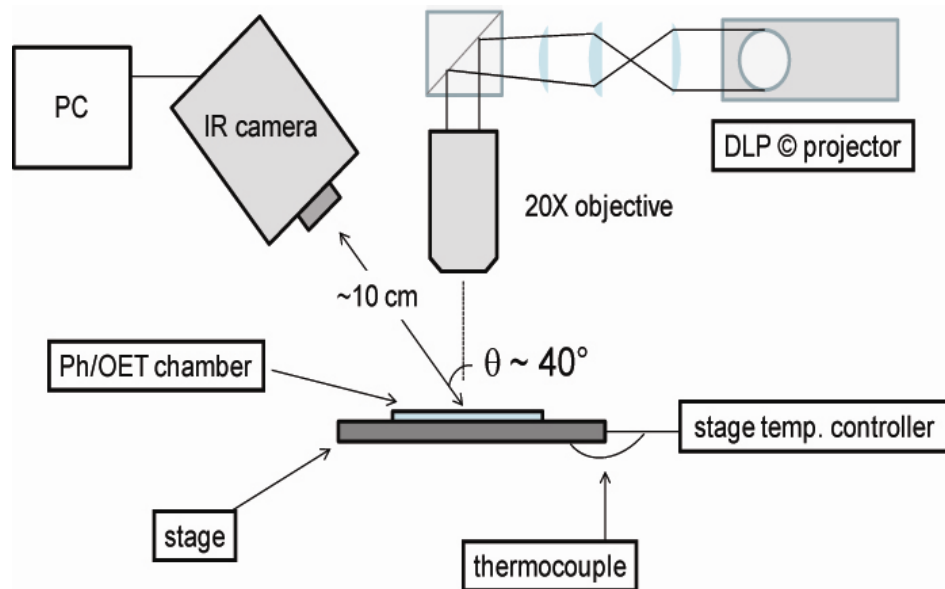


Figure 2. Block diagram of the thermography experimental apparatus (not to scale). A camera sensitive to infrared photons (3 – 5 μ m wavelength) is positioned approximately 10 cm from the PhOET device at an angle of 40°. A thermoelectric cooling stage is used to change the chamber temperature in a range from 20 to 50°C while a DLP© projector is used to create optical images for single-cell trapping through a 20x visible microscope objective lens.

The thermoelectric temperature controller maintains the stage temperature which reaches a steady state within several minutes (Figure 3A). The infrared camera records a series of sequential images throughout the temperature transition.

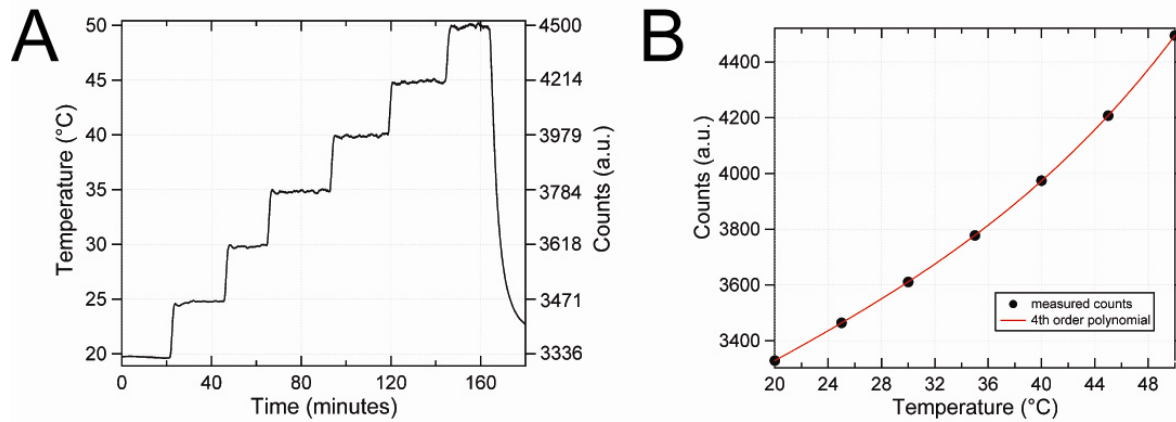


Figure 3. Typical calibration of thermographic temperature measurement. (A) Count values and calculated temperatures for a glass coverslip heated by thermoelectric temperature stage in a range from 20 to 50°C. (B) A 4th order polynomial is fit to the measured data points and used to interpolate temperature measurements during PhOET device operation.

Once the PhOET chamber reaches a steady state the camera’s count value is averaged over a circular spatial region with a diameter of approximately 5 mm for a time greater than 1 minute before adjusting the stage to the next temperature value. The average camera count value is then plotted versus the stage temperature and fit with a 4th order polynomial (Figure 3B) for use in calculating temperatures during PhOET device operation.

During PhOET device operation heating arises from two possible sources: optical absorption and Joule heating. Optical absorption normally is negligible given that the intensities used are on the order of 1W/cm² and typical spot sizes are usually 10’s of μm². Joule heating is the predominant source of heating during device operation and can be calculated with the expression:

$$Q = \sigma \times E^2 \quad (1)$$

Where “Q” represents volumetric heating [W/m³], “σ” represents the electrical conductivity [S/m], and “E” represents the electric field [V/m]. Common physiological buffers have conductivities in the range of 1.4 S/m which can lead to appreciable Joule heating at modest voltages if care is not taken to transfer the thermal load from the device. Furthermore, optical absorption can change the silicon’s photoconductivity by several orders of magnitude, locally increasing the effect of Joule heating within the absorbing thin film. The PhOET device is fabricated from a single crystalline silicon wafer with high thermal conductivity (150W/m·K) that is capable of rapidly transferring heat away from the electrolyte solution. The work presented here is aimed at measuring and controlling steady-state temperatures during normal PhOET device operation.

3. EXPERIMENTAL RESULTS

Preliminary PhOET devices were fabricated with the silicon phototransistor chip fixed to a 1 mm thick silica glass coverslip. The glass coverslip facilitates handling of the PhOET silicon-wafer, but also acts as thermal insulation given the low thermal conductivity of silica glass (1.38 W/m·K). This thermal insulation will act to restrict heat transfer out of the trapping chamber by the thermoelectric cooling stage.

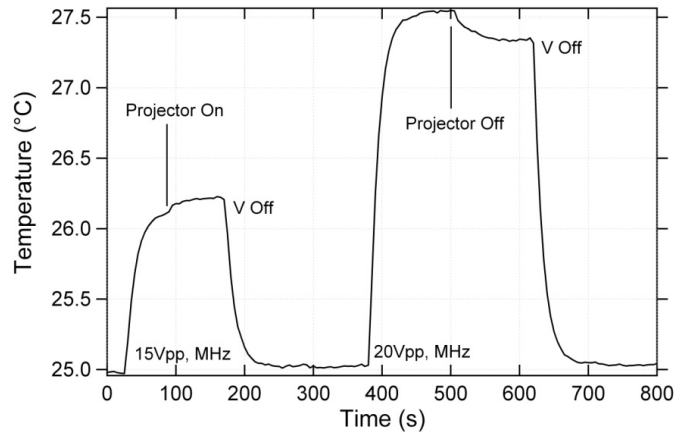


Figure 4. Temperature measurement for PhOET device supported on a glass coverslip with active thermoelectric cooling stage set to 25°C. Temperature increases on the order of 2.5°C are observed at 20Vpp, 1MHz operating conditions due to thermal insulation from the coverslip.

Given the quadratic dependence of Joule heating it is expected that device heating during operation at 20 Vpp should be $\sim 1.8 = (20/15)^2$ times larger than for operation at 15 Vpp. At 15 Vpp we measure a temperature increase of 1.2°C while at 20Vpp we measure an increase of 2.3°C, yielding a ratio of 1.9 which is in agreement with simple calculations (Figure 4). The addition of projector illumination with an optical spot diameter of 1.5 mm produced an additional temperature increase on the order of 0.2°C, which results from both optical absorption of the projector illumination as well as an increase in the conductivity of the absorbing silicon layer.

For many temperature sensitive cell lines it is desirable to control temperature increases to be less than 1°C. In order to reduce temperatures further, PhOET devices were fabricated in the absence of a thermally insulating glass coverslip with the silicon wafer placed in direct contact with the thermoelectric cooling stage. This modification is expected to remove a significant amount of resistance to heat transfer to the active cooling stage from the trapping chamber which ultimately results in lower solution operating temperatures. Data from measurements of a PhOET device in direct contact with the cooling stage are presented below (Figure 5).

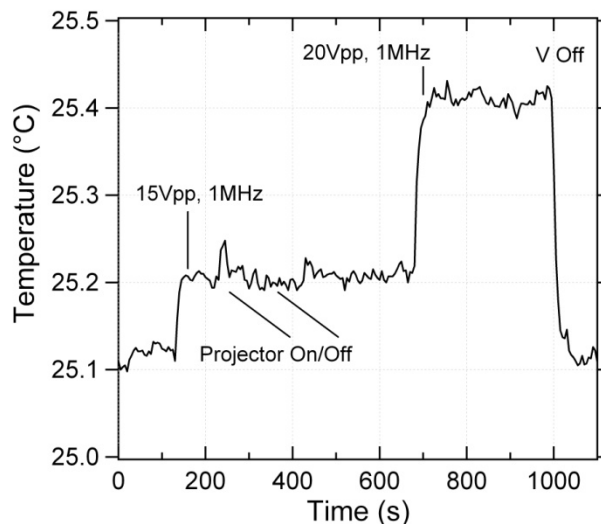


Figure 5. Temperature measurement for PhOET device in direct contact with active thermoelectric cooling stage set to 25°C. Temperature increases on the order of 0.4°C are observed at 20Vpp, 1MHz operating conditions due to removal of the thermally insulating coverslip.

Removing the glass coverslip was observed to have a dramatic impact on the PhOET device temperature. The temperature increase measured with a 15Vpp, 1MHz driving voltage was observed to be $\sim 0.1^{\circ}\text{C}$ which is ~ 10 times lower than the observed heating when there was insulation from the glass coverslip. Similarly, at 20Vpp, 1MHz the temperature increase is measured to be $\sim 0.28^{\circ}\text{C}$ which is nearly 10 times lower than the device with glass insulation. Furthermore, when light is projected within the PhOET chamber there is a brief increase in temperature by approximately 0.1°C which is rapidly compensated for by the PID stage.

4. FINITE ELEMENT SIMULATION

Finite element simulations were performed using general heat transfer and DC conductive media packages within COMSOL® to form a numerical model of experimental data. The structure consisted of sandwiched layers of ITO-coated glass, liquid media, and the silicon substrate. Both the ITO-coated glass and the silicon substrate have a diameter of 1cm, and the liquid media has a smaller diameter of 0.5cm. The temperature of the bottom of silicon substrate is fixed at 298K (25°C) due to thermoelectric cooling. Other boundaries are subjected to air convection cooling with convection coefficient $25\text{W}/(\text{m}^2\text{-K})$. The resulting temperature profile without illumination and a 20Vpp driving voltage is shown in Figure 6 and agrees well with experimental results in Figure 5. This suggests that heat transfer in the PhOET device results predominantly from Joule heating of the electrolyte solution, and can be managed effectively by relying on heat transfer through the single-crystalline silicon wafer.

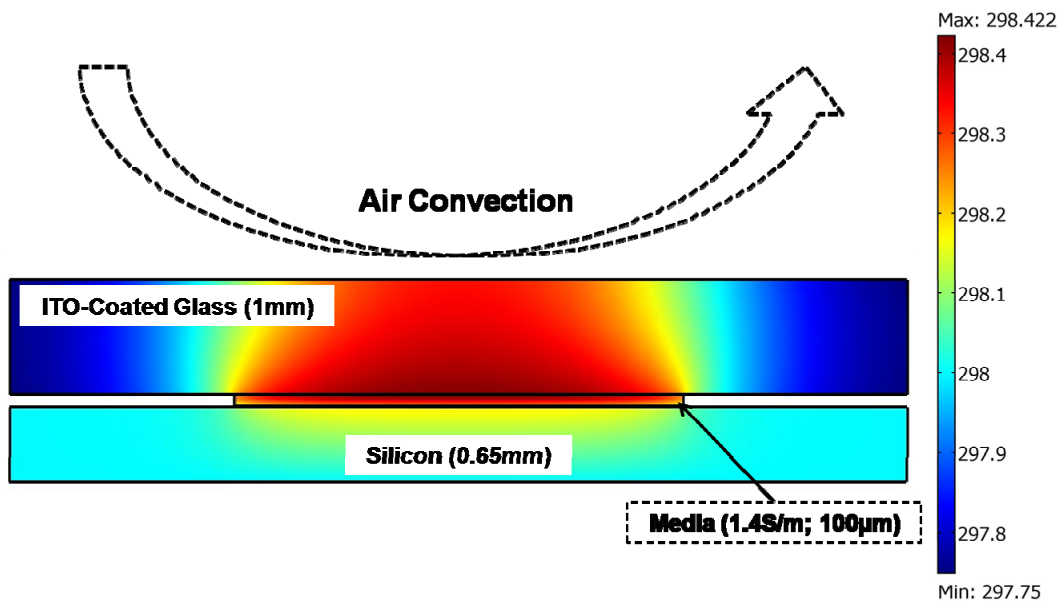


Figure 6. Finite element simulation of PhOET device without illumination during direct cooling from the thermoelectric controller stage. Temperature increases on the order of 0.5°C are calculated for the top glass surface PhOET chamber which is in agreement with observations made with the infrared camera.

CONCLUSION

Infrared thermography was used to measure temperature profiles for PhOET trapping chambers fabricated with and without glass coverslip supports. DLP® illumination was shown to have minimal heating effects at standard device operating conditions, raising device temperatures by no more than 0.2°C . Removing thermal insulation from the glass coverslip was observed to have a dramatic impact on the PhOET device temperature, ultimately limiting temperature increases below 0.5°C . Future work will focus on measuring *in situ* device temperatures with and without DLP® illumination.

ACKNOWLEDGEMENTS

The authors gratefully thank Dr. Aaron Ohta, Dr. Steven Neale, Dr. Kyoungsik Yu, and Dr. Selim Elhadj for valuable discussion. PJP acknowledges the Lawrence post-doctoral fellowship from the Lawrence Livermore National Laboratory. This work was supported in part by the NIH Roadmap for Medical Research (Grant #PN2 EY018228) and DARPA. This work was performed under the auspices of the U.S. DOE by the LLNL (Contract DE-AC52-07NA27344).

REFERENCES

- [1] Ashkin, A. Acceleration and Trapping of Particles by Radiation Pressure. *Physical Review Letters* 24, 156-& (1970).
- [2] Ashkin, A. History of optical trapping and manipulation of small-neutral particle, atoms, and molecules. *Ieee Journal of Selected Topics in Quantum Electronics* 6, 841-856 (2000).
- [3] Grier, D. G. A revolution in optical manipulation. *Nature* 424, 810-816 (2003).
- [4] Ashkin, A., Dziedzic, J. M. & Yamane, T. Optical Trapping and Manipulation of Single Cells Using Infrared-Laser Beams. *Nature* 330, 769-771 (1987).
- [5] Ashkin, A., Dziedzic, J. M., Bjorkholm, J. E. & Chu, S. Observation of a Single-Beam Gradient Force Optical Trap for Dielectric Particles. *Optics Letters* 11, 288-290 (1986).
- [6] Neale, S. L., Macdonald, M. P., Dholakia, K. & Krauss, T. F. All-optical control of microfluidic components using form birefringence. *Nature Materials* 4, 530-533 (2005).
- [7] Pauzauskie, P. J. et al. Optical trapping and integration of semiconductor nanowire assemblies in water. *Nature Materials* 5, 97-101 (2006).
- [8] Agarwal, R. et al. Manipulation and assembly of nanowires with holographic optical traps. *Optics Express* 13, 8906-8912 (2005).
- [9] Marago, O. M. et al. Femtonewton Force Sensing with Optically Trapped Nanotubes. *Nano Letters* 8, 3211-3216 (2008).
- [10] Tan, S. D., Lopez, H. A., Cai, C. W. & Zhang, Y. G. Optical trapping of single-walled carbon nanotubes. *Nano Letters* 4, 1415-1419 (2004).
- [11] Plewa, J., Tanner, E., Mueth, D. M. & Grier, D. G. Processing carbon nanotubes with holographic optical tweezers. *Optics Express* 12, 1978-1981 (2004).
- [12] Ashkin, A. & Dziedzic, J. M. Optical Trapping and Manipulation of Viruses and Bacteria. *Science* 235, 1517-1520 (1987).
- [13] Ashkin, A., Schutze, K., Dziedzic, J. M., Euteneuer, U. & Schliwa, M. Force Generation of Organelle Transport Measured In vivo by an Infrared-Laser Trap. *Nature* 348, 346-348 (1990).
- [14] Aathavan, K. et al. Substrate interactions and promiscuity in a viral DNA packaging motor. *Nature* 461, 669-U118 (2009).
- [15] Gutierrez-Medina, B., Fehr, A. N. & Block, S. M. Direct measurements of kinesin torsional properties reveal flexible domains and occasional stalk reversals during stepping. *Proceedings of the National Academy of Sciences of the United States of America* 106, 17007-17012 (2009).
- [16] Nakayama, Y. et al. Tunable nanowire nonlinear optical probe. *Nature* 447, 1098-U8 (2007).
- [17] Extermann, J. et al. Nanodoublers as deep imaging markers for multi-photon microscopy. *Optics Express* 17, 15342-15349 (2009).
- [18] Hsieh, C. L., Grange, R., Pu, Y. & Psaltis, D. Three-dimensional harmonic holographic microscopy using nanoparticles as probes for cell imaging. *Optics Express* 17, 2880-2891 (2009).
- [19] Neuman, K. C., Chadd, E. H., Liou, G. F., Bergman, K. & Block, S. M. Characterization of photodamage to *Escherichia coli* in optical traps. *Biophysical Journal* 77, 2856-2863 (1999).
- [20] Seol, Y., Carpenter, A. E. & Perkins, T. T. Gold nanoparticles: enhanced optical trapping and sensitivity coupled with significant heating. *Opt. Lett.* 31, 2429-2431 (2006).
- [21] Landry, M. P., McCall, P. M., Qi, Z. & Chemla, Y. R. Characterization of Photoactivated Singlet Oxygen Damage in Single-Molecule Optical Trap Experiments. *Biophysical Journal* 97, 2128-2136 (2009).

- [22] Liu, Y. et al. Evidence for Localized Cell Heating Induced by Infrared Optical Tweezers. *Biophysical Journal* 68, 2137-2144 (1995).
- [23] Pohl, H. A. *Dielectrophoresis* (Cambridge University Press, Cambridge, 1978).
- [24] Hughes, M. P. *Nanoelectromechanics in engineering and biology* (CRC Press, LLC, Boca Raton, 2003).
- [25] Jones, T. B. *Electromechanics of Particles* (Cambridge University Press, Cambridge, 2005).
- [26] Morgan, H. G., N.;. *AC Electrokinetics: colloids and nanoparticles* (Research Studies Press, Ltd., Philadelphia, 2003).
- [27] Fuchs, A. B. et al. Electronic sorting and recovery of single live cells from microlitre sized samples. *Lab on a Chip* 6, 121-126 (2006).
- [28] Chiou, P. Y., Chang, Z. H. & Wu, M. C. A novel optoelectronic tweezer using light induced dielectrophoresis. 2003 *Ieee/Leos International Conference on Optical Mems*, 8-9 (2003).
- [29] Chiou, P. Y., Wong, W., Liao, J. C. & Wu, M. C. Cell addressing and trapping using novel optoelectronic tweezers. *Mems 2004: 17th Ieee International Conference on Micro Electro Mechanical Systems, Technical Digest*, 21-24 (2004).
- [30] Chiou, P. Y., Ohta, A. T. & Wu, M. C. Massively parallel manipulation of single cells and microparticles using optical images. *Nature* 436, 370-372 (2005).
- [31] Neale, S. L., Mazilu, M., Wilson, J. I. B., Dholakia, K. & Krauss, T. F. The resolution of optical traps created by light induced dielectrophoresis (LIDEP). *Optics Express* 15, 12619-12626 (2007).
- [32] Ohta, A. T. et al. Dynamic cell and microparticle control via optoelectronic tweezers. *Journal of Microelectromechanical Systems* 16, 491-499 (2007).
- [33] Neale, S. L. et al. Optoelectronic tweezers (OET) trap stiffness with HeLa cells. *Proceedings of the SPIE - The International Society for Optical Engineering*, 70381K (10 pp.) (2008).
- [34] Ohta, A. T. et al. Optically controlled cell discrimination and trapping using optoelectronic tweezers. *Ieee Journal of Selected Topics in Quantum Electronics* 13, 235-243 (2007).
- [35] Hsu, H. Y. et al. Sorting of differentiated neurons using phototransistor-based optoelectronic tweezers for cell replacement therapy of neurodegenerative diseases. 15th *International Conference on Solid-State Sensors, Actuators and Microsystems. Transducers 2009*, 1598-601 (2009).
- [36] Valley, J. K. et al. Parallel single-cell light-induced electroporation and dielectrophoretic manipulation. *Lab on a Chip* 9, 1714-1720 (2009).
- [37] Jamshidi, A. et al. Dynamic manipulation and separation of individual semiconducting and metallic nanowires. *Nature Photonics* 2, 85-89 (2008).
- [38] Neale, S. L. et al. Optofluidic assembly of red/blue/green semiconductor nanowires. 2009 *Conference on Lasers and Electro-Optics (CLEO)*, 2 pp. (2009).
- [39] Jamshidi, A. et al. Semiconductor nanowire manipulation using optoelectronic tweezers. *Proceedings of the Ieee Twentieth Annual International Conference on Micro Electro Mechanical Systems, Vols 1 and 2*, 346-349 (2007).
- [40] Ohta, A. T. et al. Trapping and Transport of Silicon Nanowires Using Lateral-Field Optoelectronic Tweezers. 2007 *Conference on Lasers & Electro-Optics/Quantum Electronics and Laser Science Conference (Cleo/Qels 2007)*, Vols 1-5, 1451-1452 (2007).
- [41] Lin, Y. H., Chang, C. M. & Lee, G. B. Manipulation of single DNA molecules by using optically projected images. *Optics Express* 17, 15318-15329 (2009).
- [42] Pauzuskie, P. J., Jamshidi, A., Valley, J. K., Satcher, J. H. & Wu, M. C. Parallel trapping of multiwalled carbon nanotubes with optoelectronic tweezers. *Applied Physics Letters* 95 (2009).
- [43] Jaeger, M. S., Mueller, T. & Schnelle, T. Thermometry in dielectrophoresis chips for contact-free cell handling. *Journal of Physics D-Applied Physics* 40, 95-105 (2007).
- [44] Hsu, H. Y., Ohta, A. T., Chiou, P. Y., Jamshidi, A. & Wu, M. C. Phototransistor-based optoelectronic tweezers for cell manipulation in highly conductive solution. *TRANSDUCERS '07 & Eurosensors XXI. 2007 14th International Conference on Solid-State Sensors, Actuators and Microsystems*, 477-80 (2007).